

The climate sensitivity to human appropriation of vegetation productivity and its thermodynamic characterization

Axel Kleidon *

*Department of Geography and Earth System Science Interdisciplinary Center, University of Maryland, 2181 Lefrak Hall,
College Park, MD 20742, USA*

Received 16 March 2005; received in revised form 20 December 2005; accepted 20 January 2006
Available online 26 July 2006

Abstract

Humans appropriate terrestrial productivity to meet their food supply, their primary source of free energy. Removal of productivity from terrestrial vegetation has its direct impacts in that less energy is available for vegetation growth. Since vegetation strongly shapes the physical exchange of energy, water and momentum at the land surface, a lower ability for vegetation growth should affect this surface exchange, the overlying atmosphere, and therefore climate. Here I attempt to quantify the climate sensitivity to different intensities of human appropriation of vegetation productivity. I use sensitivity simulations with a coupled dynamic vegetation–climate system model of intermediate complexity in which I artificially remove different fractions of the simulated net primary productivity to implement human appropriation, thus reducing vegetation growth in the model. The simulations show noticeable differences in the surface energy- and water balance, with a consistent reduction in the amount of absorbed solar radiation and latent heat flux of up to 10 W m^{-2} and 27 W m^{-2} respectively and a reduction in continental precipitation by up to 30% in the global land mean when compared to the “Control” climate. However, the study also shows that mean land surface temperature is insensitive at the global scale despite pronounced regional patterns and is therefore not well suited to characterize the climatic sensitivity to land cover change at the global scale. I motivate the use of entropy production to characterize climate sensitivity. Entropy production is a thermodynamic measure of the strength of dissipative processes which perform physical work. With this measure, I show that the climate sensitivity is reflected as a clear trend towards less entropy production over land with increased intensity of human appropriation of NPP in general, and less entropy production by biotic activity in particular. I conclude that large-scale land cover changes are likely to lead to a noticeably different climate which is less favorable to biotic productivity and that this climate sensitivity is well captured by differences in entropy production as a meaningful, thermodynamic measure.

© 2006 Elsevier B.V. All rights reserved.

Keywords: terrestrial vegetation; land cover change; human appropriation; climate sensitivity; thermodynamics; entropy production

1. Introduction

Humans appropriate net primary productivity of the terrestrial biosphere (NPP) to meet their need for food resources. Human appropriated net primary productivity, or HANPP, represents the food supply for humans, providing the free energy for humans to sustain their metabolic activities and allowing them to perform physical

* Current address: Max-Planck-Institut für Biogeochemie, Postfach
10 01 64, 07701 Jena, Germany.

E-mail address: akleidon@bgc-jena.mpg.de.

URL: <http://www.earthsystem.org>.

work. HANPP also serves other purposes, such as wood use for fuel, construction, and fiber. It has been estimated that HANPP is somewhere between 10% and 55% of NPP, with a most likely value of roughly 40% (Vitousek et al., 1986, 1997; Rojstaczer et al., 2001; Imhoff et al., 2004). This removal of carbon naturally comes at a cost in that increased intensities of human appropriation should directly result in less vegetative growth compared to its natural state, if all other factors are held constant such as nutrient availability. HANPP stands for one of the primary motivations for human-driven land cover change, converting natural vegetation into agricultural systems that yield high values of HANPP. Quantifying the climate sensitivity to land cover change then translates into the question of how the removal of biotic productivity functionally alters atmosphere–biosphere interactions over land and whether this leads to consistent trends in the climate sensitivity to these modifications.

Differences in the vegetative cover impacts physical land surface functioning, and how the land surface interacts with the overlying atmosphere. For instance, a forested surface is generally characterized by its low reflectivity, is aerodynamically rough, and exhibits a high capacity to transpire moisture through an extended root system reaching deep into the soil. When converted to a pasture, several of these physical surface characteristics change. The surface associated with grass and crop cover tends to exhibit a higher reflectance, is aerodynamically smoother, and the root system does not reach as far into the soil, thus impacting the ability to transpire. Consequently, different states of the vegetated land surface affect the energy- and mass exchange over land with the overlying atmosphere, and thereby affect the climate system.

Several studies have shown that land cover change from natural vegetation to agricultural lands can have significant effects on the surface energy- and water balance and on the large-scale climate system. This has, for instance, been shown in climate model sensitivity studies to historical land cover change (e.g. Brovkin et al., 1999; Chase et al., 2000; Govindasamy et al., 2001; Bounoua et al., 2002; Defries et al., 2002; Brovkin et al., 2004) and on the potential climatic impacts of large-scale tropical deforestation (e.g. Henderson-Sellers et al., 1993; Polcher and Laval, 1994; McGuffie et al., 1995; Sud et al., 1996; Lean and Rowntree, 1997; Kleidon and Heimann, 1999). In general, these studies use maps of croplands or pastures derived either from historical sources, present-day distributions, or from scenarios of future changes. These maps are then used to prescribe the land surface properties of the modified surface, in terms of surface albedo, aerodynamic roughness, and rooting zone depth characteristic of croplands or pasture. By comparing the simulated

climate which includes human-driven land cover changes to the one representative of naturally vegetated surfaces, the climate sensitivity to land cover change is estimated. These studies generally point out that the climate over land is sensitive in that the components of the energy- and water balance differ among the simulations. However, when the climate sensitivity of land cover change is integrated in terms of temperature differences to the global scale, a common problem is that temperate and high-latitude regions generally show a cooling trend while tropical regions tend to show strong warming. In the global average, therefore, the climate sensitivities cancel out at the global scale despite the noticeable climatic differences (e.g. Hansen et al., 1998; IPCC, 2001).

In this paper, I derive the climate sensitivity to land cover change using a novel approach that is based on HANPP. I then show that the resulting climate sensitivity is not well captured by global mean temperature, but results in a clear trend in thermodynamic variables.

To model the effects of human-driven land cover change, I implement human appropriation into a climate model of intermediate complexity. In that model, NPP is “diverted” to human use which is then unavailable for vegetation growth. The strength of appropriation is characterized by a parameter f_{hanpp} which describes the fraction of productivity diverted to HANPP, i.e. $\text{HANPP} = f_{\text{hanpp}} \text{NPP}$. With this definition of f_{hanpp} , the case of natural vegetation is represented by $f_{\text{hanpp}} = 0$ and would likely lead to the highest vegetation growth ($\text{GROW} = \text{NPP}$) and biomass, but no human appropriation ($\text{HANPP} = 0$). Greater values of f_{hanpp} will inevitably result in less relative vegetation growth and biomass. At a certain point, the reduction in biomass is likely to impact the ability of the vegetative cover to absorb light and extract water from the soil, thus reducing the ability to be productive. The extreme case of $f_{\text{hanpp}} = 100\%$ represents the case in which all vegetation productivity is diverted to human use. Consequently, no biomass can be produced, overall vegetation productivity should be close to zero, and $\text{HANPP} \approx 0$. This simple consideration of extremes points out that we can expect a maximum in HANPP to exist at an intermediate value of f_{hanpp} (Fig. 1, top). Note that this consideration only considers the effect of standing biomass on productivity. Factors such as increased availability of nutrients in human-dominated systems or irrigation from groundwater, which increase productivity independent of biomass, are not considered here.

Different levels of vegetation biomass in turn affect land surface properties, such as surface albedo, roughness, and rooting zone depth, and thereby climate. We can then pose three contrasting hypotheses regarding the associated climate sensitivity to f_{hanpp} (Fig. 1, bottom): our null

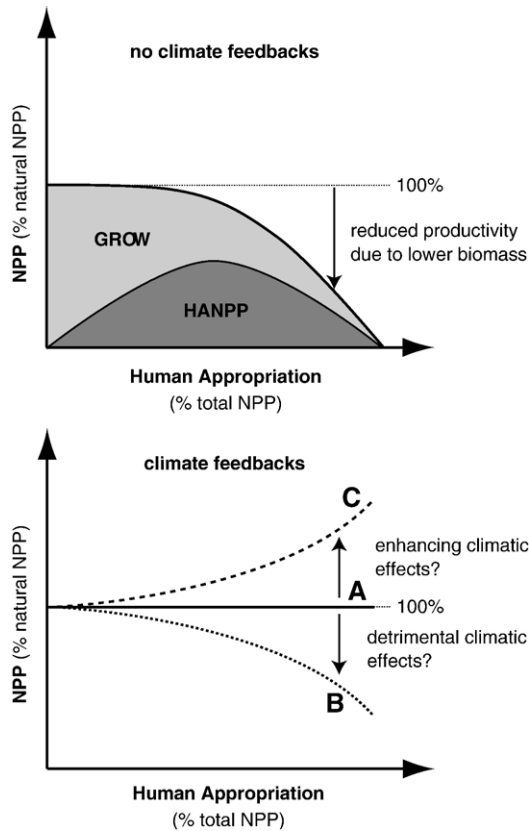


Fig. 1. Conceptual diagram to illustrate the hypothetical response of vegetation productivity (NPP, net primary productivity) to different intensities of human appropriation. The top figure refers to the isolated effect of reduced biomass on vegetation productivity due to less growth, resulting in less biomass. The lower figure illustrates three possible changes in the climatic conditions under which vegetation performs photosynthesis. Case “A” shows a neutral response, where the removal of NPP may affect climatic conditions, but in no consistent direction. Case “A” represents the null hypothesis for this study. In case “B”, the removal of NPP leads to climatic conditions that are less favorable to photosynthesis, whereas case “C” represents the case in which climatic conditions would be more favorable to photosynthesis.

hypothesis is case A where different intensities of f_{hanpp} may affect climate, but not in a consistent fashion that impacts the climatic potential for vegetation productivity. An alternative hypothesis is case B in which increasing values of f_{hanpp} lead to a “degraded” climate, that is, it leads to climatic conditions that allow for reduced rates of vegetation productivity. This response has been found for the extreme case of a “Desert World” climate, in which the climatic conditions would only allow for substantially reduced rates of vegetation productivity (Betts, 1999; Fraedrich et al., 1999; Kleidon et al., 2000; Kleidon, 2002). The third possible response is case C in which increasing values of f_{hanpp} would lead to climates that are more suitable to vegetation productivity. Again, other

factors which raise productivity independent of climatic conditions are not considered here.

I evaluate the two responses shown in Fig. 1 with a coupled dynamic vegetation–climate system model. I introduce the formulation of HANPP described above into the SimBA dynamic vegetation model, which is part of the Planet Simulator, an Earth system model of intermediate complexity (Lunkeit et al., 2004; Fraedrich et al., 2005b). SimBA simulates vegetation productivity as a function of the prevailing environmental conditions. Vegetation productivity in turn leads to biomass build-up, which then translates into land surface properties. A brief description of the climate model, a more detailed description of the vegetation model, and the way how the parameter f_{hanpp} is introduced in the model is described in Section 2.

I then perform coupled climate–vegetation model simulations in which I vary f_{hanpp} in a globally uniform fashion, which, while artificial, is used here to demonstrate the concepts shown in Fig. 1. This allows me to continuously vary the extent of large-scale land cover change through different values of f_{hanpp} . Through the use of f_{hanpp} , I shift the emphasis for evaluating the climate sensitivity to human-driven land cover change from what it “looks like” to what it “does”. The sensitivity simulations are then evaluated in terms of differences in the surface energy- and water balance over land, and in terms of how suitable the climatic conditions are for vegetation productivity in Section 3.

The discussion section (Section 4) points out potential limitations in terms of the method used to implement land cover change, the resulting climate differences, and compares the climate sensitivity to previous studies. Furthermore, it is discussed why mean surface temperature is of little use in characterizing the climate sensitivity for the simulations performed here. Instead, I suggest an evaluation of climate sensitivity in terms of differences in the dissipative nature of climate processes over land, as characterized by entropy production, and how these impact the ability of the terrestrial biosphere, and humans in particular, in performing physical work. This paper closes with conclusions and suggestions of how this study can be extended in the future.

2. Methods

2.1. The climate model

This study uses sensitivity simulations with an Earth system model of intermediate complexity, the Planet Simulator (Lunkeit et al., 2004; Fraedrich et al., 2005a). The atmospheric component consists of a low resolution

atmospheric general circulation model with T21 spectral resolution (corresponding to a grid resolution of about $5.6^\circ \text{ lon} \times 5.6^\circ \text{ lat}$). It includes prognostic calculations of radiative transfer and the atmospheric water cycle including a predictive cloud scheme. The version used here uses 10 atmospheric layers. The atmospheric component is coupled to a simple land surface model, a mixed-layer ocean model with prescribed heat transport and a dynamic sea-ice model. Land surface parameters are dynamically calculated by a dynamic vegetation model. The model is freely available, runs on standard desktop computers, and can be downloaded at http://www.mi.uni-hamburg.de/Planet_Simulator.216.0.html.

2.2. The dynamic vegetation model

The Simulator for Biospheric Aspects (SimBA) is a simplified dynamic parameterization of terrestrial vegetation. The main purpose of SimBA is to predict large-scale, land surface properties that are affected by the presence of vegetation dynamically from the prevailing climatic conditions. SimBA simulates these as follows. The atmospheric and land surface conditions as simulated by the climate model set the constraints for the gross carbon uptake, or gross primary productivity (GPP) by the vegetation. GPP leads to biomass buildup, which in turn affects land surface parameters, specifically surface albedo a_s , aerodynamic roughness length z_0 , and rooting zone depth W_{max} . These in turn affect land surface energy- and mass exchange in the climate model. SimBA code is executed at every time step of the physical model code of the Planet Simulator.

In the following, an abbreviated description of SimBA is given, focussing on the main equations in order to understand how vegetation interacts with the climate system within the Planet Simulator, and how human appropriated NPP is included into the model formulation. For a more detailed description of SimBA, see Lunkeit et al. (2004).

The main state variable of SimBA is vegetation biomass C_{veg} . Vegetation biomass results from the balance of carbon uptake by photosynthesis and release by respiration. The calculation of GPP is based on Monteith's approach, expressing GPP as the minimum of a light- and water limited rate (Monteith et al., 1989; Dewar, 1997; Kleidon, 2004c). The light-limited rate $\text{GPP}_{\text{light}}$ is expressed using a light use efficiency approach:

$$\text{GPP}_{\text{light}} = \epsilon_{\text{luc}} \cdot f(T_s) \cdot g(p\text{CO}_2) \cdot f_{\text{leaf}} \cdot \text{SW} \quad (1)$$

where ϵ_{luc} is a globally uniform light use efficiency, $f(T_s)$ a function that decreases productivity for cold temperatures (with T_s being the surface temperature),

$g(p\text{CO}_2)$ the dependence of productivity on $p\text{CO}_2$, f_{leaf} the fraction of the surface covered by leaves ("leaf cover"), and SW the amount of solar radiation absorbed at the surface. The exchange flux of carbon through the leaf stomata is associated with water loss that leads to transpiration. The associated carbon flux $\text{GPP}_{\text{water}}$ is calculated from the rate of evapotranspiration ET as:

$$\text{GPP}_{\text{water}} = c_{\text{CO}_2} \cdot \frac{p\text{CO}_{2,a} - p\text{CO}_{2,l}}{q_{\text{sat}}(T_s) - q_a} \cdot \text{ET} \quad (2)$$

where $p\text{CO}_{2,a} - p\text{CO}_{2,l}$ is the gradient in carbon dioxide across the leaf–air interface (taken to be 70% of the atmospheric $p\text{CO}_2$ concentration of $p\text{CO}_2 = 360$ -ppm), $q_{\text{sat}}(T_s) - q_a$ is the specific humidity gradient across the leaf–air boundary, and c is a constant which includes the lower diffusivity of CO_2 in relation to water vapor and other conversion factors. The motivation behind Eq. (2) is that dividing ET by the specific humidity gradient yields the exchange coefficient needed to determine the CO_2 flux into the leaf. For simplicity, it is assumed that the total evaporative flux from the land surface is controlled by vegetation. Evaporation from the bare soil and from intercepted water in the canopy is neglected in the model.

Vegetation biomass is determined from the balance of GPP, autotrophic respiration, and litter production. It is assumed that 50% of GPP is respired by autotrophic respiration through plant growth and maintenance, so that the net primary productivity is $\text{NPP} = 0.5 \cdot \text{GPP}$. A fixed ratio of NPP to GPP is commonly observed and can be understood by optimum nitrogen allocation in canopies, Dewar (1996). Litter production F_{litter} is assumed to be proportional to C_{veg} and characterized by a typical residence time τ_{veg} . Thus, the time evolution of C_{veg} is described by:

$$\frac{dC_{\text{veg}}}{dt} = (1 - f_{\text{hanpp}}) \cdot \text{NPP} - \frac{C_{\text{veg}}}{\tau_{\text{veg}}} \quad (3)$$

Eq. (3) includes the parameter f_{hanpp} , which, as discussed in the Introduction, characterizes the human appropriation of NPP (with $0 \leq f_{\text{hanpp}} < 1$). That is, only $\text{GROW} = (1 - f_{\text{hanpp}}) \text{NPP}$ is allocated to vegetation biomass growth, while

$$\text{HANPP} = f_{\text{hanpp}} \cdot \text{NPP} \quad (4)$$

is the human appropriated portion of NPP. With this formulation, a value of $f_{\text{hanpp}} = 0$ translates into the case of natural vegetation in which no NPP is appropriated for human consumption as explained in the Introduction.

Land surface parameters are derived from vegetation biomass C_{veg} , which is used to parameterize the effects

of structural vegetation biomass, and leaf area index LAI, capturing the effect of leaf display on land surface shape and functioning. LAI in turn is computed as a function of biomass and soil water availability. These two parameters are converted into fractional covers of vegetation f_{veg} and green leaves f_{leaf} by

$$f_{\text{veg}} = \frac{1}{C_c} \cdot \arctan\left(\frac{C_{\text{veg}} - C_a}{C_b}\right) + C_d \quad (5)$$

and

$$f_{\text{leaf}} = 1 - \exp(-k \cdot \text{LAI}) \quad (6)$$

where c_a , c_b , c_c , and c_d are empirical parameters derived from observations, and $k=0.5$.

The fractional covers are used to express land surface properties as functions of a value representative of a fully vegetated and bare, non-vegetated surface. Surface albedo in the absence of snow is expressed as:

$$a_s = a_{\text{veg}} \cdot f_{\text{leaf}} + a_{\text{nonveg}} \cdot (1 - f_{\text{leaf}}) \quad (7)$$

with $a_{\text{veg}}=0.12$ is the albedo value used to represent a fully vegetated surface and $a_{\text{nonveg}}=0.30$ is the corresponding value used for a bare surface. In the presence of snow, the surface albedo a_s is parameterized as a function of f_{veg} in order to capture the structural effects of forests on the snow albedo (e.g. Bonan et al., 1992):

$$a_s = a_{\text{snow,veg}} \cdot f_{\text{veg}} + a_{\text{snow,nonveg}} \cdot (1 - f_{\text{veg}}) \quad (8)$$

where $a_{\text{snow,nonveg}}=0.4\text{--}0.8$ is the simulated albedo of snow cover in the absence of vegetation (which depends

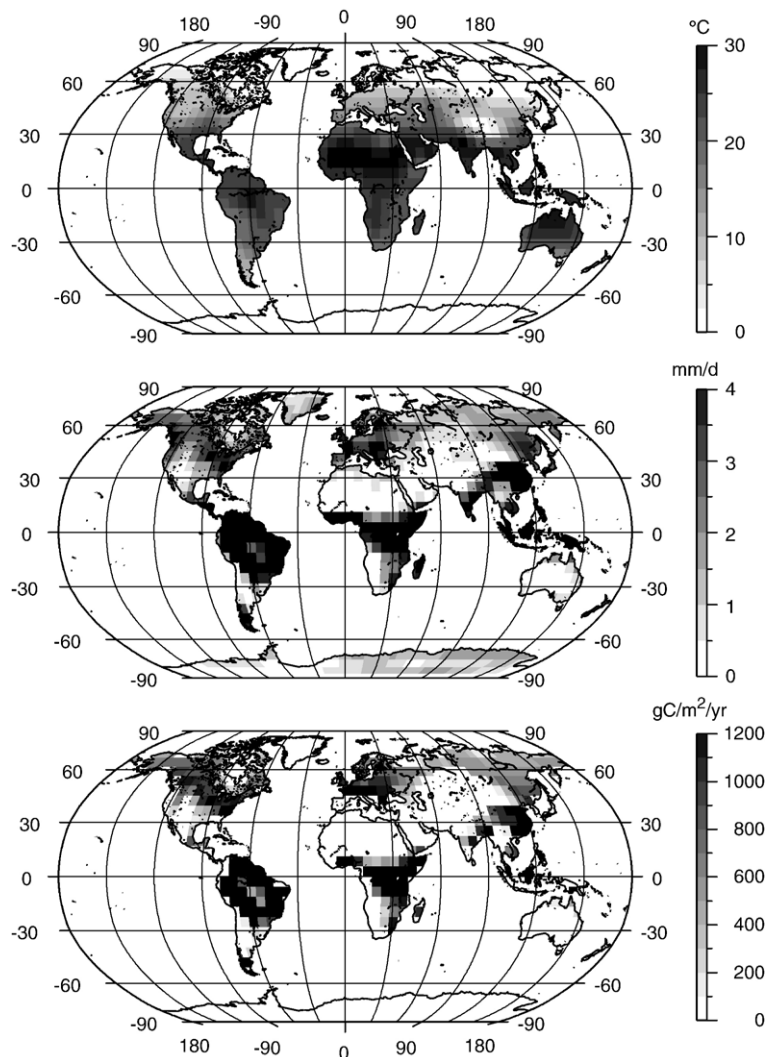


Fig. 2. Simulated annual mean values over land for temperature (top), precipitation (middle), and net primary productivity (bottom) for the Planet Simulator's "Control" setup.

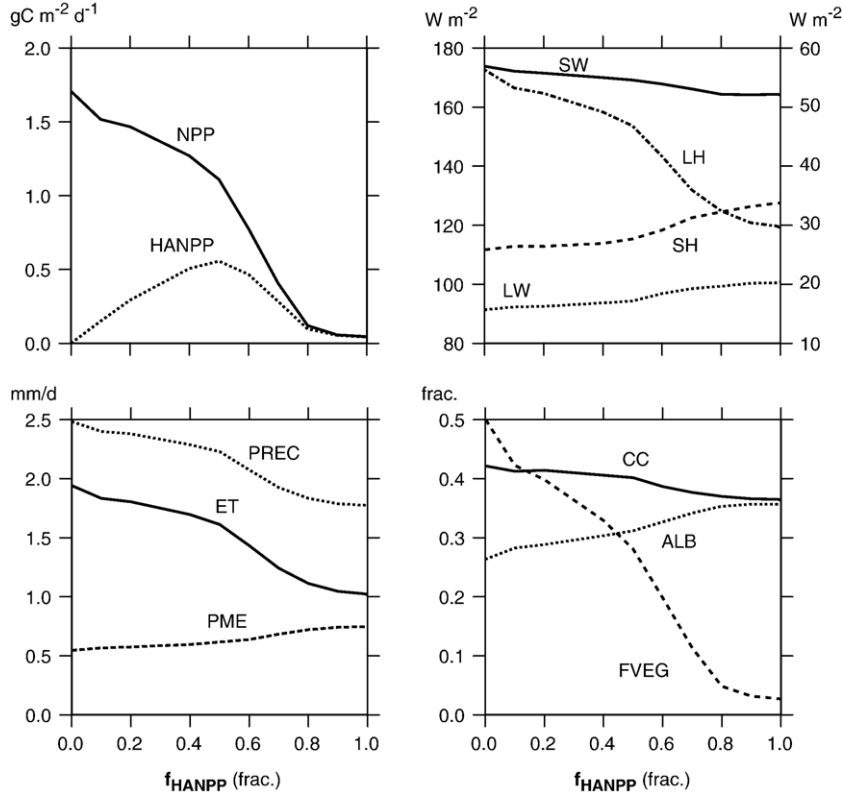


Fig. 3. Annual mean land averages for different values of the fraction of human appropriated net primary productivity (f_{HANPP}). Top left: net primary productivity (NPP) and human appropriated NPP (HANPP). Top right: absorbed shortwave (SW, left scale) and net emission of longwave (LW, left scale) radiation at the surface and sensible (SH, right scale) and latent (LH, right scale) heat flux. Bottom left: precipitation (PREC), evapotranspiration (ET), and atmospheric moisture convergence $\text{PME} = \text{PREC} - \text{ET}$. Bottom right: cloud cover (CC), surface albedo (ALB) and fractional vegetation cover (FVEG).

on surface temperature) and $\alpha_{\text{snow,veg}} = 0.35$ the albedo of a fully vegetated surface with snow cover. The surface roughness length $z_{0,\text{srf}}$ and the soil water holding capacity of the rooting zone W_{max} are derived in a similar fashion from f_{veg} by:

$$z_{0,\text{srf}} = z_{0,\text{veg}} \cdot f_{\text{veg}} + z_{0,\text{nonveg}} \cdot (1 - f_{\text{veg}}) \quad (9)$$

and

$$W_{\text{max}} = W_{\text{max,veg}} \cdot f_{\text{veg}} + W_{\text{max,nonveg}} \cdot (1 - f_{\text{veg}}) \quad (10)$$

where $W_{\text{max,nonveg}} = 50$ mm, $W_{\text{max,veg}} = 500$ mm (taken as a typical value from Kleidon, 2004b), $z_{0,\text{nonveg}} = 0.05$ m and $z_{0,\text{veg}} = 2$ m are the corresponding values for a bare and fully vegetated surface respectively. Overall surface roughness is derived by combining orographic roughness $z_{0,\text{oro}}$ with the surface roughness $z_{0,\text{srf}}$ using $z_0 = \sqrt{z_{0,\text{oro}}^2 + z_{0,\text{srf}}^2}$.

The set of Eqs. (1)–(10) capture the essence of the SimBA model. Eqs. (1)–(3) link the climate variables T_s , $p\text{CO}_2$, and ET with carbon uptake GPP and biomass

C_{veg} . Biomass and leaf display in turn affect land surface parameters as described by Eqs. (8)–(10). Thus, these equations form an interactive system, where the climatic conditions affect vegetation productivity, which

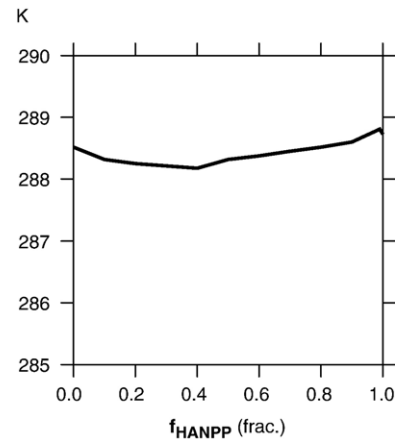


Fig. 4. Sensitivity of annual mean land temperature to f_{HANPP} .

Table 1

Global land averages of vegetation and climatic properties for the “Control” simulation ($f_{\text{hanpp}}=0.0$), the “HANPP_{max}” simulation at which HANPP is at a maximum ($f_{\text{hanpp}}=0.5$), and the “Desert” simulation ($f_{\text{hanpp}}=1.0$)

Simulated variable	Control	HANPP _{max}	Desert
Net primary productivity ($\text{gC m}^{-2} \text{d}^{-1}$)	1.71	1.11	0.04
HANPP ($\text{gC m}^{-2} \text{d}^{-1}$)	0.00	0.56	0.04
Absorbed SW (W m^{-2})	173.8	169.2	164.2
Net emission LW (W m^{-2})	91.4	94.4	100.6
Sensible heat (W m^{-2})	25.8	27.6	33.7
Latent heat (W m^{-2})	56.3	46.9	29.5
Precipitation (mm d^{-1})	2.49	2.23	1.76
Evapotranspiration (mm d^{-1})	1.94	1.61	1.01
Near surface temperature (K)	288.5	288.3	288.7
Cloud cover (frac.)	0.42	0.40	0.36
Surface albedo (frac.)	0.26	0.31	0.36
Vegetation cover (frac.)	0.50	0.28	0.03

in turn affects land surface parameters, and thereby the climatic conditions. The steady-state properties of the coupled vegetation–climate system emerging for different prescribed values of f_{hanpp} , in terms of the surface energy- and water balance and simulated fluxes of NPP and HANPP, are evaluated by long model integrations as described in the following subsection.

2.3. Coupled model simulation setup

A range of model simulations is conducted for values of $f_{\text{hanpp}}=0.0, 0.1, 0.2, 0.3, 0.4, 0.5, 0.6, 0.7, 0.8, 0.9$ and 1.0 . In each simulation, a value of f_{hanpp} is prescribed globally uniform so that no regional variations in the relative removal of NPP are considered here. While this seems somewhat artificial, this setup was chosen here as a first step to demonstrate the concept and show consistent climatic impacts for the range of specified values. The “Control” simulation is represented by $f_{\text{hanpp}}=0.0$. The other extreme of $f_{\text{hanpp}}=1.0$ represents the case in which all growing vegetation is instantaneously removed, thus leading to a scenario close to the one of a world with a “Desert” surface. The simulation in which HANPP is at a maximum will be referred to as “HANPP_{max}” in the following.

In the simulations, values for maximum stomatal conductance and canopy roughness were used which maximize GPP in the control simulation (Kleidon, 2004c). This setup was chosen because it leads to a realistic partitioning of the surface energy balance that is consistent with ECMWF reanalysis (Pavlick and Kleidon, submitted for publication). Each simulation

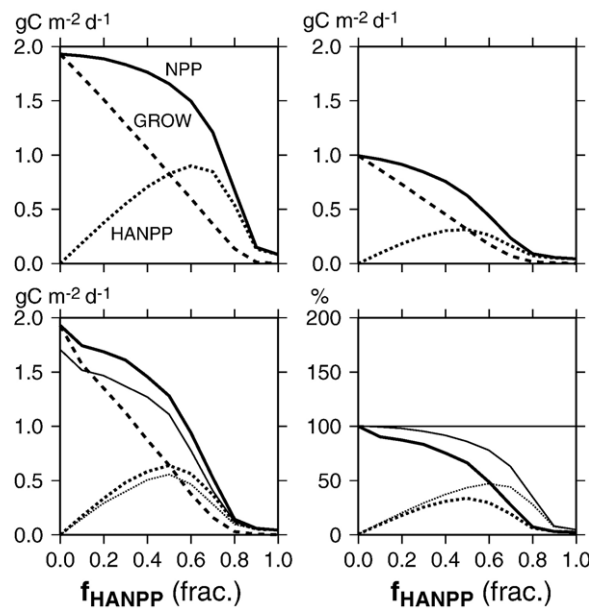


Fig. 5. Analysis of the relative effects of biomass reduction vs. climatic conditions on the sensitivity of NPP to f_{hanpp} with the standalone version of the dynamic vegetation model. Top left: model sensitivity of NPP (solid), HANPP (dotted), and GROW (dashed) using the prescribed “Control” climate in all simulations. Top right: same as (top left), but with the prescribed “Desert” climate. Bottom left: same as (top left), but with the prescribed climates of the corresponding simulation of the coupled model, with the thin lines being the corresponding sensitivity of the coupled model from Fig. 3. Bottom right: summary of attribution of NPP decline due to biomass alone (thin lines) and the combined effect of biomass and climate (thick lines), with 100% representing the NPP for the “Control” climate.

was conducted for a period of 100 years to allow the coupled dynamic vegetation–climate system to come close to a steady state. The last 10 years were used for the analysis and compared to the control simulation.

All simulations are run with prescribed, climatological sea-surface temperatures and sea-ice cover. The concentration of atmospheric carbon dioxide is prescribed to a fixed concentration of 360 ppm. The carbon flux of HANPP is not returned into the model, so that the carbon balance over land is not closed. These simplifications are justified here as the primary focus of this study is on the direct climatic effects of land cover change on land surface climate. The potential implications of these limitations, however, need to be kept in mind in the interpretation of the results.

The simulated “Control” climate shows reasonable distributions of annual mean temperature, precipitation and vegetation productivity as shown in Fig. 2.

2.4. Standalone model simulation setup

In order to separate the effects of biomass reduction from the climatic effects on productivity (cf. Fig. 1), additional sets of sensitivity simulations were performed with a standalone version of the vegetation model. In a first set of simulations, the sensitivity

simulations to f_{hanpp} are repeated but with the prescribed climate of the “Control” simulation. A comparison to the interactive simulations with the coupled model then provides an estimate of the isolated effects of biomass reduction. This set of simulations is repeated, but using the prescribed climate of the “Desert” simulation. A final set of simulations was performed in which each standalone simulation was forced with the respective climate of the interactive simulation. This latter set of simulations should ideally reproduce the sensitivity of the fully coupled model. A comparison with the coupled model simulations then reveals biases resulting from the standalone setup.

Each simulation of the stand-alone model is run for 100 years, with the last 10 years used for analysis. The standalone version of the model runs on a daily time step, using daily forcing from the last 10 years of the climate model simulations.

3. Results

3.1. Global land averages

The results of the sensitivity simulations are shown in terms of their global land averages in Fig. 3. With an increased value of f_{hanpp} , overall productivity NPP

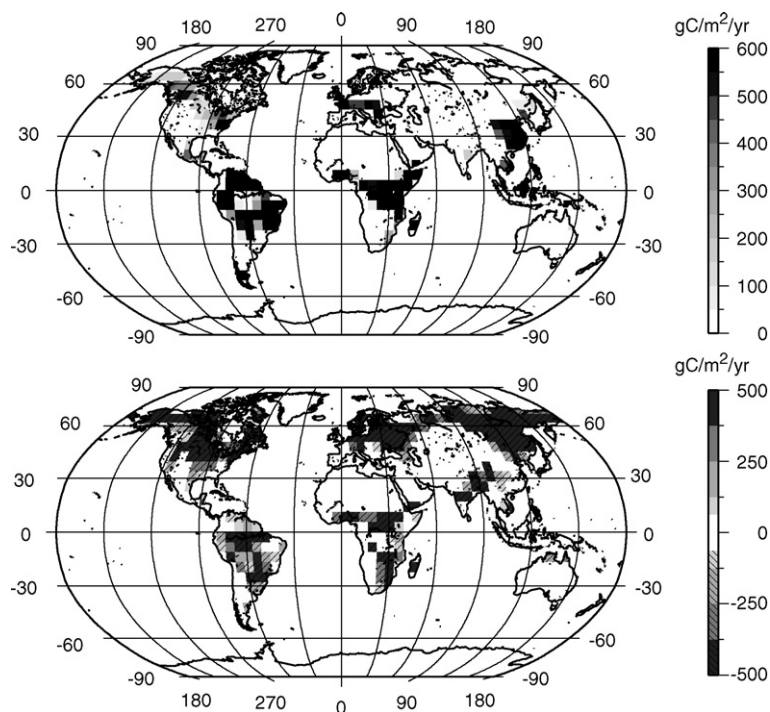


Fig. 6. Geographic distribution of HANPP for the “HANPP_{max}” simulation (top) and difference in NPP between the simulation “HANPP_{max}” and the “Control”.

decreases smoothly up to about $f_{\text{hanpp}}=50\%$ beyond which it declines more steeply to close to zero NPP for values above $f_{\text{hanpp}}=80\%$. The amount of HANPP increases with f_{hanpp} up to $f_{\text{hanpp}}=50\%$ beyond which it is reduced as a result of the general decrease in NPP.

A reduction in (NPP–HANPP) leads to less available carbon for growth, less vegetation biomass and vegetative cover, and consequently altered land surface characteristics. These altered surface properties lead to a substantial reduction in land surface evapotranspiration (ET) and the associated latent heat flux, impacting the surface energy- and water balance over land. This reduction is compensated by an increase in net emission of longwave radiation and the sensible heat flux with increasing values of f_{hanpp} , and a reduction in overall absorption of shortwave radiation. Reduced ET leads to less recycling of water over land, thus reducing precipitable water (not shown) and continental precipitation (PREC), although the reduction in PREC is less than the reduction in ET. This means that the net atmospheric moisture convergence over land (PREC–ET), and hence continental runoff ($R=\text{PREC}-\text{ET}$), increases with f_{hanpp} in the model simulations. While these climatic differences are quite substantial, the global land surface temperature

hardly differs among the simulations (Fig. 4)). The reason for this seemingly inconsistent model behavior is investigated in detail in Section 3.3 below as well as in the discussion (Section 4.3).

Note that overall absorption of shortwave radiation at the surface decreases despite a general decrease in cloud cover. This is the consequence of the model's overall behavior, where the decrease in cloud cover is more than compensated by the increase in surface albedo, therefore resulting in the decrease in absorbed shortwave radiation with higher values of f_{hanpp} .

A change in slope in the global means can be seen at $f_{\text{hanpp}}=0.5$, which coincides with the maximum in HANPP. This change in slope is attributable to the non-linear mapping of vegetation biomass into fractional vegetation cover (Eq. (5)). At high biomass values, f_{veg} changes little with decreasing biomass resulting from $f_{\text{hanpp}}>0$, hence resulting only in minor climatic differences. When increased values of f_{hanpp} reach a steady-state biomass values of $C_{\text{veg}}=c_a$, the slope of $df_{\text{veg}}/dC_{\text{veg}}$ is highest, therefore resulting in a steeper decline in f_{veg} and stronger impacts on the simulated climate. As discussed in the Introduction, it is this non-linearity that shapes the maximum in HANPP. The occurrence of this maximum in the simulation with

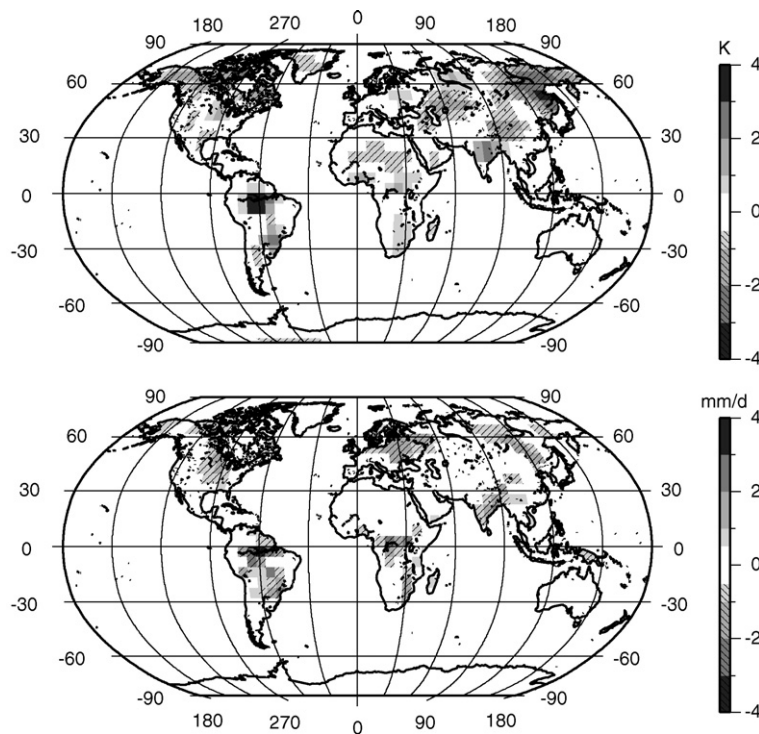


Fig. 7. Differences in annual mean near surface temperature (top) and precipitation (bottom) between the simulation “HANPP_{max}” and the “Control”. Hatched areas denote negative differences.

$f_{\text{hanpp}}=0.5$ is closely related to the transition point characterized by c_a , and is therefore sensitive to the particular choice of c_a .

Table 1 summarizes the climate sensitivity to f_{hanpp} for the two extreme simulations “Control” and “Desert” as well as for the intermediate simulation “HANPP_{max}”.

3.2. Relative effects of climatic and biomass differences on simulated NPP

The results shown in Fig. 3 represent the combined response of reduced biomass and altered climatic conditions that result in the overall reduction in NPP. The separation of the two effects with the standalone model simulations are shown in Fig. 5. The comparison of the modelled sensitivity of the standalone version of the vegetation model reproduces a reasonable pattern compared to the sensitivity of the coupled model, although both NPP and HANPP are slightly overestimated in the standalone version of the model (as shown in the lower left of Fig. 5).

The sensitivity of NPP and HANPP to f_{hanpp} in the absence of climatic effects (i.e. with the prescribed “Control” climate) shows that both, NPP and HANPP are generally higher compared to the coupled model simulations. This shows that the climate effects amplify

the sensitivities, representing case B in Fig. 1. Also noticeable is a shift in the maximum value of HANPP, which occurs at a slightly higher value of $f_{\text{hanpp}}=0.6$ rather than $f_{\text{hanpp}}=0.5$ in the coupled simulations. The reduced climatic potential for productivity is also displayed for the extreme case when the “Desert” climate is prescribed to the sensitivity simulations. The simulated productivity consistently is reduced roughly by a factor of two. This means that the “Desert” climate is “half as suitable” for productivity in terms of its climatic constraints than the “Control” climate.

In terms of the relative effects of biomass reduction vs. climatic differences, a shift occurs in their relative importance towards higher values of f_{hanpp} . At small values of f_{hanpp} we notice that the biomass reduction has a relatively small effect, while most of the reduction in NPP results from climatic differences. For instance, for $f_{\text{hanpp}}=0.2$, the biomass reduction reduces NPP to 98% compared to the “Control”, while the combined effects (climate difference+biomass reduction) reduce it to 87%. The relative importance of biomass reduction in reducing NPP in the simulations increases with increasing f_{hanpp} . At $f_{\text{hanpp}}=0.5$, biomass reduction yields a decrease in NPP to 86% while the combined effects yields a decrease to 66%. At $f_{\text{hanpp}}=0.8$, NPP is reduced to 35% and 7% respectively.

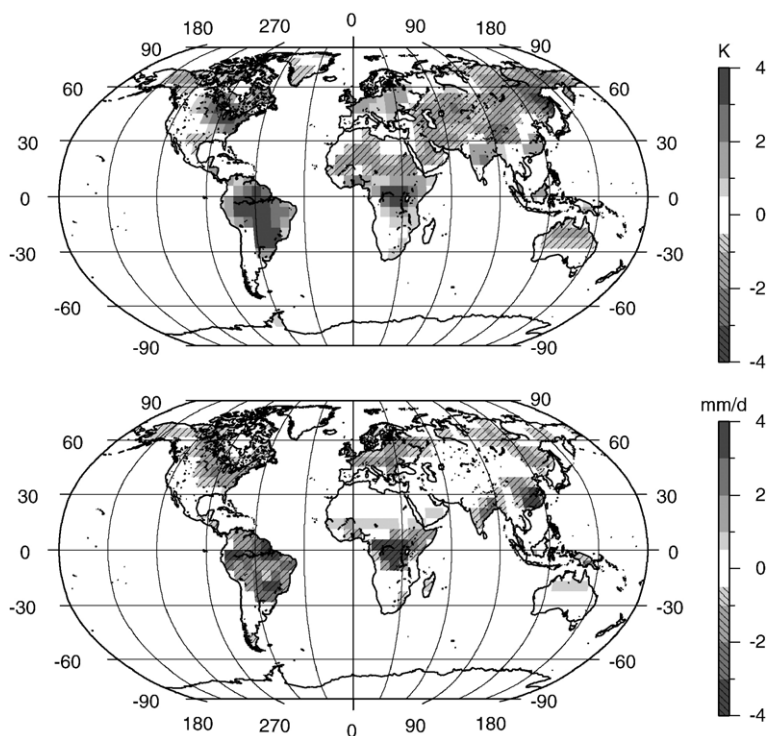


Fig. 8. Same as Fig. 7 but for the difference between the simulations “Desert” and the “Control”.

In summary, this analysis points out that both factors, reduced biomass and climatic differences, contribute substantially to the overall reduction in NPP, with the reduced climatic potential for NPP best captured when the standalone model is run with the “Desert” climatic forcing.

3.3. Geographic variations

The geographic variation of annual mean HANPP in the “HANPP_{max}” simulation and the associated reduction in overall NPP in comparison to the “Control” is shown in Fig. 6. High values of HANPP are concentrated in those regions where NPP is high in the Control simulation (Fig. 2). Adjacent regions in the more arid subtropics and the cold, high latitudes show a strong decline in NPP, thus resulting in little HANPP. What this points out is that while $f_{\text{hanpp}}=0.5$ may maximize HANPP in highly productive regions and in the global mean in the model, the optimum value for f_{hanpp} is likely to be lower in the more constrained regions of the higher latitudes and subtropics.

The geographic variation of climatic differences of the simulations “HANPP_{max}” and “Desert” in comparison to the “Control” simulation are shown in Figs. 7 and 8 for annual mean temperature and precipitation. The differences in annual mean temperature show consistent patterns for the two simulations, with the “Desert” simulation showing a greater magnitude in difference. In both cases, strong warming is found over the tropical regions of South America and tropical Africa, compared to a general cooling in the higher latitudes. Also, a consistent cooling can be seen in both simulations over the Saharan desert in Africa and the Arabic peninsula. The response in the mid-latitudes shows no clear response in the “HANPP_{max}” simulation, but a clearer pattern emerges in the “Desert” simulation, with strong warming in eastern North America and Western Europe, and a cooling in central Asia. Differences in precipitation show similar patterns in both simulations, with a general decrease of precipitation found in areas of high precipitation.

The contrasting responses in temperature sensitivity in the tropics and extratropics originates from two primary effects that reduced vegetation cover has on the local surface energy balance: a reduced ability to transpire water, and the increase of surface albedo, particularly during periods when snow is present. The reduction in ET is a relevant driver for temperature differences in regions and during periods of high solar radiation where sufficient precipitation is potentially available to meet the evaporative demand. The seasonal differences clearly show this effect, as shown in Fig. 9 for the simulation “HANPP_{max}” and in Fig. 10 for the simulation “Desert”.

In the northern hemisphere extratropics, this effect is restricted to the summer months, and leads to a warming in the zonal seasonal means in the “Desert” simulation (but note the differing responses along the same latitude that is shown in Figs. 7 and 8). The second effect results from the increase of surface albedo in the presence of snow when forest cover is reduced (Bonan et al., 1992). This effect is most pronounced during the spring season, as reflected in the strong reduction in absorbed SW radiation (MAM in Figs. 9 and 10). This reduction of spring-time heating then corresponds to the period of strongest cooling in the northern hemisphere. The fact that a general cooling in the northern hemisphere extratropics in the annual mean is shown in Figs. 7 and 8 then implies that the spring-time cooling trend is stronger than the summertime warming trend due to reduced ET.

What this latter analysis points out is that differences in annual mean temperature are not particularly well suited to characterize the climatic impacts of human land

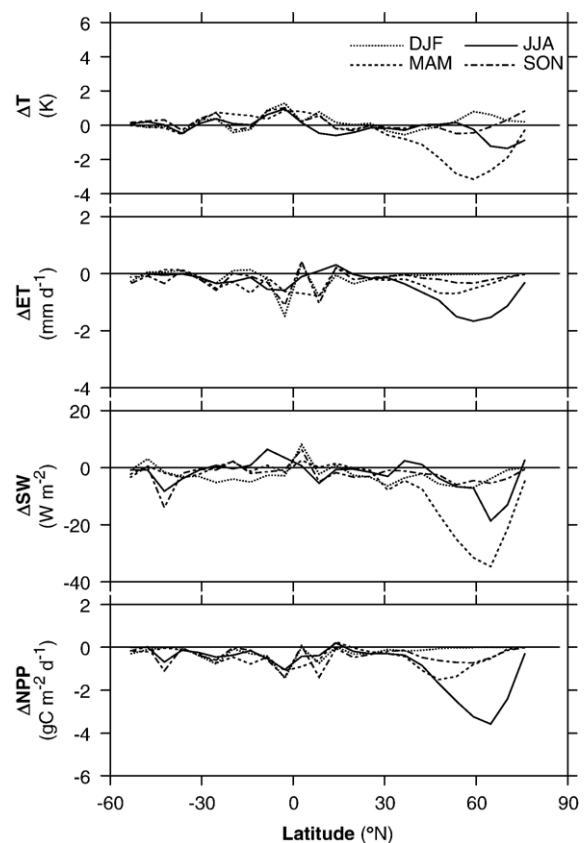


Fig. 9. Zonally averaged seasonal differences between the simulation “HANPP_{max}” and the “Control”. From top to bottom: 2 m air temperature, evapotranspiration, absorbed shortwave radiation at the surface, and NPP. Zonal averages were taken over land regions only.

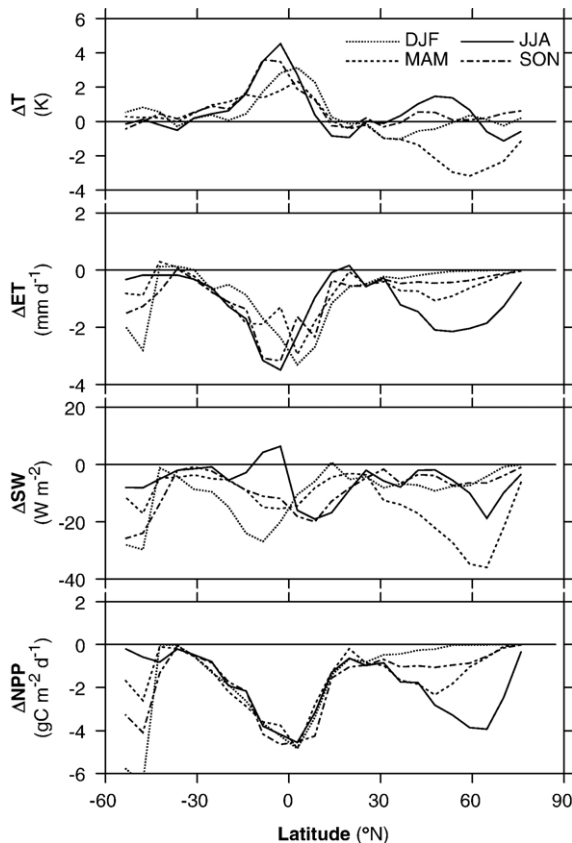


Fig. 10. Same as Fig. 9 but for the difference between the simulations “Desert” and the “Control”.

surface modification in these simulations. This is even more apparent when the climatic differences in temperature are averaged over all land regions (as in Fig. 4), where the cooling in the extratropics compensates for the warming found in the tropics, thus yielding no global land surface temperature sensitivity to f_{hanpp} . Yet, the climatic differences lead to clear and consistent declines in NPP with increased f_{hanpp} , as shown in Figs. 7 and 8. A broader perspective on why NPP is a well-suited measure for climate impacts is discussed in more detail in Section 4.3 below.

4. Discussion

In this discussion section, I focus on four themes. I first point out limitations of the study and compare the results to previous studies in Section 4.1. The comparison to previous studies will show that the results reported here are consistent, so that they are unlikely to be strongly impacted by these limitations. This comparison also shows that the novel approach of modeling land cover change presented here leads to

reasonable results. I then discuss in more depth why an overall decline in NPP with increasing f_{hanpp} is a reasonable trend to be expected (Section 4.2). This is followed by a discussion why mean surface temperature does not characterize climate sensitivity well (Section 4.3) and why a general perspective on the dissipative nature of land surface processes, and biotic productivity and its human appropriation is a more meaningful measure of climate sensitivity (Section 4.4).

4.1. Limitations and comparison to previous studies

The results of the study are naturally subject to limitations. I focus on the discussion of limitations due to deficiencies resulting from (i) the simple parameterizations used in model, (ii) the simulation setup, including how the use of HANPP was implemented to model land cover change, and (iii) potential biases in terms of the simulated climatic impacts associated with different intensities of f_{hanpp} .

4.1.1. Limitations due to model parameterizations

The model used in this study is clearly of “intermediate complexity”, meaning that the formulations of climate system processes and terrestrial vegetation are quite simplistic and many details are being left out. Yet, many aspects of the simulated climatic differences are consistent with previous studies. For instance, the spring-time cooling associated with the reduction in boreal forest cover is similar to the study of Bonan et al. (1992). Also, a moderate cooling in mid-latitudes for moderate values of f_{hanpp} is found in the simulations here, in agreement with previous studies of Bonan (1997), Hansen et al. (1998), Brovkin et al. (1999), Govindasamy et al. (2001), Defries et al. (2002), Brovkin et al. (2004), and Oleson et al. (2004). The climate differences in the tropics, particularly the reduction in ET and the increase in surface temperature, are consistent with previous sensitivities to large-scale tropical deforestation (e.g. Shukla et al., 1990; Henderson-Sellers et al., 1993; Sud et al., 1996; Lean and Rowntree, 1997; Kleidon and Heimann, 1999).

Furthermore, the extreme climate of the “Desert” simulation compares very well to our previous study (Kleidon et al., 2000), in terms of the conceptual setup and in terms of the differences in the simulated climates. Yet, the climate model used here differs greatly in its complexity from the one used in the previous study. Kleidon et al. (2000) used the ECHAM-4 GCM, a climate system model of high complexity and prescribed fixed land surface characteristics of a desert surface in their simulation. Table 2 shows the overall importance

of terrestrial vegetation on the land climate in terms of the difference between the “Control” and “Present-Day” climates in comparison to those of a “Desert World” for the two studies. The differences in the surface energy balance components are remarkably close in magnitude and direction: both studies report an overall increase in the absorption of shortwave radiation at the surface with natural vegetation (despite an increase in cloud cover in both studies, not shown), both show a decrease in net emission of longwave radiation and sensible heat, and a substantial increase in evapotranspiration. The fact that two quite different models yield very similar estimates should increase our confidence in the overall mechanism by which terrestrial vegetation moderates the large-scale climate, how large-scale land cover changes impact climate when natural vegetation is removed, and how the climatic potential for vegetation productivity declines with these conversions (as shown in Fig. 3, Table 1, and by Kleidon, 2002).

4.1.2. Limitations due to model setup

The focus here was on large-scale climatic differences as a result of uniform levels of land cover change. Aspects associated with landscape heterogeneity at a smaller scale as a result of land cover transformations as well as scaling its effects up to the GCM grid box scale has not been considered here. Also, in some regions irrigation can have a noticeable effect on the local- to regional climate, but the effect of irrigation has not been considered here as well. Furthermore, the simulations conducted here were run without an interactive ocean and without an interactive carbon cycle. Previous studies by Bonan et al. (1992) and Claussen et al. (2001) have shown that those feedbacks can be of importance and can modify the overall response to some extent. This study

can be extended in the future to account for these two important aspects.

Using HANPP as a starting point to model human-driven land cover change has been implemented here rather conceptually and leaves many aspects that can be improved. In the simulations, the intensity of human appropriation of NPP was prescribed by one, globally uniform parameter f_{hanpp} . This is quite clearly unrealistic, but was helpful in the setup here in order to quantify the overall climate sensitivity on a continuous scale and to demonstrate the existence of a maximum in HANPP. As pointed out in the Results section, it is likely that the optimum value for f_{hanpp} varies for different regions, for instance with likely smaller values for boreal regions. This would suggest that the overall maximum value of HANPP is likely to be underestimated. This may then in turn lead to a different overall climate difference between the “Control” and the “HANPP_{max,local}” simulations, with “HANPP_{max,local}” being a simulation in which the maximization of HANPP with respect to f_{hanpp} is conducted at every grid point, rather than in a globally uniform fashion.

The lack of consideration of anthropogenic inputs of nutrients also would likely lead to an underestimation of both HANPP and NPP.

4.1.3. Limitations of simulated sensitivity

It is likely that the overall decline in NPP is overestimated in this study for the following reasons. In the model formulation, any decrease in GROW (or NPP) leads to a direct reduction in biomass, and hence leads to different land surface parameters. This parameterization is somewhat simplistic in that it does not account for adaptive shifts, for instance in the allocation patterns within the vegetation that would potentially be able to compensate for decrease in GROW to some extent. Furthermore, while vegetation in the “Control” simulation was taken to be optimally adapted to its environment, optimal adaptation to altered climates in the sensitivity simulations was not considered (see also below). Under altered climatic conditions, the vegetative cover is likely to adapt, for instance with respect to its stomatal conductance and its partitioning of carbohydrates to above- vs. belowground growth. This would inevitably lead to a bias in which the sensitivity of NPP to f_{hanpp} would be overestimated (as also pointed out in Kleidon, 2004a).

In summary, it would seem that overall, the method used to model human land cover modifications through HANPP and the associated climate sensitivity obtained here seem sufficiently realistic despite the potential imitations and biases discussed above. In light of these

Table 2

Comparison of the overall effect of natural vegetation on the climate system as determined here from the extreme simulation “Desert” and from the study by Kleidon et al. (2000) (with additional information taken from Kleidon, 2004a)

Simulated variable	“Control”–“Desert”	“Present-Day”– “Desert World”
	(this study)	(Kleidon et al., 2000)
Absorbed surface SW (W m^{-2})	+10	+6
Net emission surface LW (W m^{-2})	–9	–12
Sensible heat (W m^{-2})	–8	–5
Latent heat (W m^{-2})	+27	+26
Precipitation (mm d^{-1})	+41%	+52%

limitations, the results and the analysis presented here should be seen as a proof of concept and a first step.

4.2. Decline in NPP — to be expected?

I motivated this study in the Introduction with a conceptual diagram of what to expect when the intensity of human appropriation of NPP increases (Fig. 1). The proposed existence of a maximum in HANPP is clearly evident in Fig. 3, although its value may to some extent be underestimated by the limitations discussed above. Furthermore, I outlined three possible responses of how the climatic conditions for NPP differ with $f_{\text{hanpp}} > 0$. The results reported here are consistent with case B shown in Fig. 1. The simulated climatic conditions are becoming increasingly less suitable for NPP with increased values of f_{hanpp} , as shown with the standalone sensitivity simulations with the vegetation model. This can be attributed to the general decrease in precipitation in most of the tropics and mid-latitudes, thus increasing the water limitation of productivity, and the general decrease in spring-time temperatures which decreases the length of the growing season in temperature-limited regions of the higher latitudes.

The decrease in NPP with increasing values of f_{hanpp} is to be expected for the following reason. The reference climate used in this study (the “Control” simulation) is one in which vegetation productivity is at a maximum under the prevailing climatic constraints. This is equivalent to the notion that natural vegetation is optimally adapted to its environment. The success of such an implementation has been demonstrated in previous studies. For instance, Kleidon and Heimann (1998) and Kleidon (2004b) show that the maximization of NPP yields realistic predictions of the geographic variation of rooting zone depth. At a more fundamental level, maximization of NPP is consistent with the notion that the rate of entropy production of complex systems is maximized in steady state, subject to the relevant constraints imposed on the system (see e.g. overviews by Ozawa et al., 2003; Kleidon and Lorenz, 2005a,b; see also discussion in Section 4.4 below).

The maximization of productivity in the “Control” climate is the result of a balancing between the light- and water limited rates of photosynthesis. When both rates are the same (i.e. $\text{GPP}_{\text{light}} = \text{GPP}_{\text{water}}$, see Eqs. (1) and (2)), then overall GPP is at a maximum. The “Control” climate here uses vegetation parameters, specifically stomatal conductance, which are adjusted such that these two limiting rates are balanced and vegetation productivity is maximized (Kleidon, 2004c). When this climate–vegetation steady-state is disturbed by removal of NPP by

human appropriation, the resulting climate is then likely to be associated with a shifted balance between these two limitations. Consequently, one of these fluxes is likely to become more limiting than the other, and thus overall NPP is decreased.

As already mentioned above, adaptation in vegetation to this shifted balance could compensate for this decline in NPP to some extent, and therefore reduce the overall climate sensitivity. Additional simulations would be necessary to estimate the potential magnitude of this compensation. This could be done by conducting the optimization of vegetation parameters for each of the prescribed values of f_{hanpp} . This is, however, beyond the scope of this study.

4.3. Mean surface temperature as a measure of climate sensitivity

Differences in mean surface temperature are generally reported to characterize the overall impact of differences in climatic forcings. Particularly in studies of global climatic change due to elevated concentrations of CO_2 , the climate sensitivity is generally discussed with respect to differences in mean surface temperature, and, closely associated, radiative forcing (e.g. Hansen et al., 1998, IPCC, 2001). As pointed out by Pielke et al. (2002), Marland et al. (2003) and this study, mean surface temperature or radiative forcing are not a particularly well-suited choice to characterize the climate sensitivity to land cover change. This study represents the extreme case, in which substantial climatic differences over land are found, yet the global mean land surface temperature is insensitive to these differences.

The dilemma which arises when characterizing climate sensitivity by differences in mean surface temperature can be illustrated by the consideration of the simplified steady-state surface energy balance in the climatic mean:

$$0 = \text{SW} + \text{LW}_{\downarrow} - \sigma T_s^4 - \text{SH} - \text{LH} \quad (11)$$

where SW is the amount of absorbed solar radiation at the surface, LW_{\downarrow} the downward flux of terrestrial radiation (i.e. the radiative forcing of the atmospheric greenhouse), σT_s^4 is the emission of terrestrial radiation from the surface (with a temperature T_s and σ being the Stefan–Boltzmann constant) and SH and LH ($= \lambda \cdot \text{ET}$) are the sensible and latent heat fluxes respectively. The two terms that are directly driven by T_s are the emission term σT_s^4 and the sensible heat flux SH.

In the case of elevated atmospheric concentrations of CO_2 , LW_{\downarrow} increases and this leads to additional heating of the surface. This is in steady state compensated for by

an increase in temperature ($\Delta T > 0$), which raises the fluxes that remove energy from the surface. The characterization of this driver of climatic change by differences in ΔLW_{\downarrow} or ΔT is therefore straightforward.

However, when considering alterations in the land cover, changes in the energy balance are not as straightforward. Modifying the vegetated cover results in a reduction in SW – due to the increase in surface albedo – and in a reduction in LH – due to the decreases in leaf cover, surface roughness and rooting zone depth. Surface roughness also affects the atmospheric motion over land, and thereby the larger-scale transport of heat and moisture. For matters of simplicity, this aspect is neglected in the following discussion, although it is included in the model simulations.

In a simple, first-order line of reasoning, the reduction in SW by itself would lead to less heating, and should result in a cooling (i.e. $\Delta T < 0$). Less LH by itself would lead to less cooling, and should result in a warming ($\Delta T > 0$). What the insensitivity of mean surface temperature in our model simulations indicates is that the reduction of heating due to the albedo increase is approximately of the same magnitude as the reduction of cooling due to the decrease in the latent heat flux in the global mean over land.

The differing response in temperature for tropics vs. northern latitudes can be understood by the relative proportion of ΔSW compared to ΔLH , which is shown in Figs. 9 and 10. Noting that a reduction of 1 mm/d in ET leads to a corresponding reduction in LH of about 30 W m^{-2} , one can directly estimate the contrasting radiative forcings. For the “Desert” simulation, we find for instance a reduction in ET of about 3–4 mm/d in the tropics, corresponding to a reduction in surface cooling of about $90\text{--}120 \text{ W m}^{-2}$. Compared to this drastic reduction in surface cooling, the differences in SW are relatively minor, so that a net warming $\Delta T > 0$ results. In contrast, in the northern latitudes during the spring season, ET is reduced by less than 1 mm/d, reducing the surface cooling by less than 30 W m^{-2} , while the reduction in SW is up to 40 W m^{-2} . Thus, in the northern hemisphere spring season, the reduction of SW heating outweighs the reduction in LH cooling, thus resulting in a surface cooling $\Delta T < 0$. The resulting ΔT is therefore delicately sensitive to the relative difference in surface heating and cooling terms, which in turn depends on the geographic region, but also on the details of the model parameterization (e.g. assumed values of rooting depth change vs. surface albedo change; the importance of the relative change has for instance been reported in sensitivity simulations to tropical deforestation by Dirmeyer and

Shukla (1994), Lean and Rowntree (1997), and Kleidon and Heimann (2000)).

In other words, the climatological energy balance can, in principle, be solved in many different ways with the same surface temperature as an outcome. The associated solutions differ, however, in their suitability for vegetation productivity, so that surface temperature by itself is insufficient to characterize the impacts of land cover change on the land surface climate.

4.4. Entropy production and climate sensitivity

The previous two subsections show that while mean surface temperature is not a good measure for the climate sensitivity, NPP shows a clear and consistent trend towards lower values with increasing f_{hanpp} and seems to be well suited to characterize the climate sensitivity to land use change. Here, I motivate the use of entropy production as a metric of climate sensitivity, a measure that provides a deeper insight of why NPP reflects the climate sensitivity so well.

Entropy production is the consequence of dissipative, irreversible processes. In the Earth system, dissipative processes degrade energy from the low entropy nature of solar radiation to subsequently higher entropy, which is eventually expelled to space by the emission of high entropy terrestrial radiation (e.g. Peixoto et al., 1991; Kleidon and Lorenz, 2005a). The entropy balance of Earth supplements the energy balance by providing important information about the physical work done by dissipative processes. In steady state, the rate at which work is being performed is balanced by the rate of dissipative heating, which in turn is linked to entropy production by $D = \sigma_{\text{diss}} T_{\text{diss}}$ with σ_{diss} being the rate of entropy production by the dissipative process and T_{diss} the temperature at which the dissipation occurs. In this consideration of entropy production, I neglect complicating factors and focus on mean temperatures and fluxes to estimate rates of entropy production. This simplification surely impacts the accuracy on the validity of the analysis. A full treatment of the entropy budget requires an inclusion of entropy calculations within the climate model that allows for instantaneous evaluations of entropy fluxes and production. While this is possible (e.g. Kleidon and Lorenz, 2005b), it is not the focus of this study. The following discussion should therefore be viewed as a motivation for future work along these lines.

The question that is addressed in the following is whether differences in human-driven land cover, as expressed by f_{hanpp} , lead to a consistent trend in the overall dissipative behavior of the climate system

over land. If this is the case, differences in entropy production can be used as a metric to characterize climate sensitivity.

I calculate rough estimates of the mean rates of entropy production over land following Peixoto et al. (1991), using the global averages shown in Table 1. In addition, I also estimate entropy production associated with activity by the terrestrial biosphere and humans σ_{bio} and σ_{hanpp} respectively. Strictly speaking, σ_{hanpp} represents the entropy production due to the dissipation of human appropriated carbohydrates. Dissipation of free energy derived from other sources, particularly fossil fuels, is not considered here. For σ_{bio} , we need to estimate the production of free energy associated with photosynthetic activity which is then subsequently dissipated by respiring carbohydrates. Photosynthesis is a photochemical process that is driven by the absorption of shortwave photons. At a minimum, it requires 8 photons of ≈ 700 nm wavelength to fix one molecule of CO_2 (the quantum yield efficiency, e.g. Larcher, 1995). I use this maximum in quantum yield efficiency and estimate that 1426 kJ of photons is required to fix one mol of carbon. Using this number in combination with the simulated values of GPP yields the overall energy flux Q_{bio} associated with photosynthetic activity on land. In steady state, this energy flux is dissipated by photorespiration, autotrophic respiration, and heterotrophic respiration roughly at a temperature T_s . This is then used to estimate the overall biotic entropy production by $\sigma_{\text{bio}} = Q_{\text{bio}}(1/T_s - 1/T_{\text{sun}})$ following Kleidon (2004a) and Kleidon and Fraedrich (2005). In this expression, T_{sun} is the emission temperature of the Sun $T_{\text{sun}} = 5760$ K and characterizes the low entropy nature of solar radiation that is needed for photosynthesis. Consequently, σ_{bio} is essentially proportional to GPP. For σ_{hanpp} I use $\sigma_{\text{hanpp}} = D/T_s$. The rate of dissipation D is taken to be 479 kJ/mol C, which is the amount of free energy in carbohydrates (Larcher, 1995), times the carbon flux of HANPP.

The differences in entropy production compared to the “Control” simulation are shown in Fig. 11. Naturally, the overall trends shown are similar to those in Fig. 3, yet Fig. 11 does not show energy fluxes *per se*, but the intensity of the associated degradation of energy to higher entropy. What Fig. 11 shows is an overall decline in the rate of entropy production with increasing values of f_{hanpp} , dominated by the decrease associated with reduced absorption of shortwave radiation, but also by decreases in biotic activity (i.e. lower rate of photosynthesis and, therefore, respiration, although this contribution is already included in σ_{sw}) and in the latent heat fluxes. This decline is only marginally compensated for by an

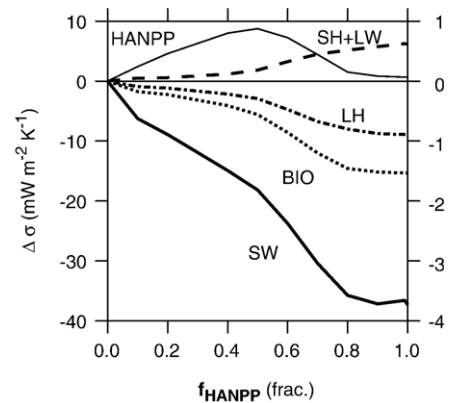


Fig. 11. Sensitivity of annual mean land averages of entropy production rates to f_{hanpp} . Shown are differences in the rate of entropy production $\Delta\sigma$ for different dissipative processes: absorption of shortwave radiation (total, at surface and in the atmosphere, SW, solid line); absorption of longwave radiation and sensible heat flux (SH + LW, combined in dashed line); latent heat flux (LH, dash-dotted line); biotic activity (BIO, dotted line); and human consumption of NPP (HANPP, thin solid line, right axis).

increase in entropy production by sensible heat and absorption of longwave radiation. Thus, the climate system over land becomes overall less dissipative with increasing f_{hanpp} .

The clear trend of decreasing σ_{bio} with f_{hanpp} has been explained above in terms of decreasing biomass and shifts in the limitations imposed by light and water on vegetation productivity (see Section 4.2). The overall reduction in entropy production with increasing f_{hanpp} (i.e. less vegetation) is consistent with the hypothesis that the presence of life acts to increase, or even maximize, the rate of entropy production by climate system processes subject to the relevant constraints (Ulanowicz and Hannon, 1987; Kleidon, 2004a).

The entropy production σ_{hanpp} associated with HANPP and its subsequent dissipation follows exactly that shown in Fig. 3. The difference here, again, lies in its interpretation. It is not shown as a carbon flux, but as a dissipative flux, that is, it is associated with the ability of humans to perform physical work, at least to the extent to which this is driven by NPP as the source of free energy. The direct purpose of human-driven land use change is also well characterized by σ_{hanpp} , that is, its role as a source of free energy. This then leads to a natural trade-off: when more energy is diverted away from vegetation growth to human consumption, it enhances human activity, but this comes at a cost of overall reduced level of biotic activity. The existence of a maximum in HANPP leads to the interpretation that this would allow the anthroposphere (that is, totality of

all humans) to perform maximum work. In this sense, σ_{hanpp} could also be viewed as a measure of “human habitability” of a certain climatic environment. Note that heat loss from the human body may act as another relevant climatic constraint on “human habitability” that is not considered here (Kleidon, submitted for publication).

The consideration of entropy production at the land surface suggests that, in general, processes perform less physical work with increasing f_{hanpp} . More importantly for overall extent of biotic activity, the climatic conditions change with increasing f_{hanpp} that allow for less biotic work to be done (i.e. lower potential for growth and reproduction). This could be interpreted as the climate becoming less habitable. It would seem that the ability of the biota to perform work, and entropy production rates in general, are much more meaningful measures of climate sensitivity than the traditional measure of global mean surface temperatures. However, the estimates computed here are rather rough, and more work needs to be done in order to provide more detailed estimates of entropy production and its response to climatic change. It is nevertheless a first step towards classifying climate and climate sensitivity not merely by differences in the energy balance, but rather in terms of dissipative processes that are more relevant to biotic and human activity.

5. Summary and conclusions

In this paper, I presented a novel approach to simulate the effects of human modifications to the land surface and their consequences for the climate system. Instead of prescribing land surface characteristics representative of the modified land cover in sensitivity simulations, I characterized the human impacts on large-scale land surface functioning by their removal of a fraction of vegetation productivity. I then conducted a range of sensitivity simulations with a coupled vegetation–climate model in which I varied the intensity of human appropriation of productivity and demonstrated significant climatic differences that follow a consistent trend. The overall climate sensitivity in these simulations is not well captured when evaluated in terms of differences in the global mean surface temperature. I then introduced entropy production as a measure of the intensity of different dissipative processes over land. The climate sensitivity viewed from this thermodynamic perspective showed a relatively clear and unambiguous trend, with a reduction in entropy production with increasing intensity of human appropriation of productivity.

What I conclude from this analysis is that: (i) the new approach used here to describe human modifications of the natural land surface by their appropriation of net primary productivity leads to a robust climate sensitivity that is consistent with previous studies, particularly regarding the contrasting effects on surface temperature for tropical and temperate/boreal regions; (ii) the use of entropy production provides a thermodynamic perspective of climate sensitivity and seems to lead to a better characterization of the climate sensitivity to land use change than the traditional approach of using differences in global mean surface temperature; and (iii) that entropy production is in fact a more meaningful overall measure of climate sensitivity than mean surface temperature. It provides direct information about how much work is being performed by climate system processes over land, and, as a result, how much energy is dissipated to a degraded form. It is meaningful because it characterizes climate sensitivity not by how much warming or cooling occurs, but rather by how much the suitability to perform physical work differs — by physical dissipative processes such as the turbulent exchange of the surface and the atmosphere, and by the activity of the terrestrial biosphere and anthroposphere. When using mean surface temperature to characterize climate sensitivity, we are plagued by the ambiguity in the interpretation of temperature effects: for instance, a warming can lead to a lower surface albedo due to earlier snowmelt, more absorption in solar radiation, and higher productivity in the boreal region while the same warming in a tropical environment may enhance the vapor pressure deficit, reduce productivity and leaf area, and therefore increase surface albedo. Thus, depending on the geographic location, warming can result in more or less absorption of solar radiation at the surface, and can lead to differing responses for vegetation productivity. When viewed from a thermodynamic perspective, if climatic change enhances the potential for entropy production, it has a clear implication: more physical work can be done. Furthermore, entropy production provides a unifying perspective of seemingly different processes in the climate system (energy vs. water vs. carbon fluxes) and it is well suited in that it provides a clear reference point defined by states of maximum entropy production (e.g. Paltridge, 1978; Grassl, 1981; Ozawa and Ohmura, 1997; Shimokawa and Ozawa, 2002; Lorenz et al., 2001; Ozawa et al., 2003; Kleidon et al., 2003, 2006; Kleidon and Fraedrich, 2005). This thermodynamic interpretation of climate sensitivity would seem worthy of further development and applications to other topics related to global climatic change.

Acknowledgments

The author thanks Richard Betts and one anonymous reviewer for their constructive reviews of this manuscript. This work is partially supported by the National Science Foundation through grant ATM 513506.

References

- Betts, R.A., 1999. Self-beneficial effects of vegetation on climate in a ocean–atmosphere general circulation model. *Geophys. Res. Lett.* 26, 1457–1960.
- Bonan, G.B., 1997. Effects of land use on the climate of the United States. *Clim. Ch.* 37, 449–486.
- Bonan, G.B., Pollard, D., Thompson, S.L., 1992. Effects of boreal forest vegetation on global climate. *Nature* 359, 716–718.
- Bounoua, L., DeFries, R., Collatz, G.J., Sellers, P., Khan, H., 2002. Effects of land cover conversion on surface climate. *Clim. Ch.* 52, 29–64.
- Brovkin, V., Ganopolski, A., Claussen, M., Kubatzki, C., Petoukhov, V., 1999. Modelling climate response to historical land cover change. *Glob. Ecol. Biogeogr.* 8, 509–517.
- Brovkin, V., Sitch, S., von Bloh, W., Claussen, M., Bauer, E., Cramer, W., 2004. Role of land cover changes for atmospheric CO₂ increase and climate change during the last 150 years. *Glob. Chang. Biol.* 10, 1253–1253.
- Chase, T.N., Pielke, R.A., Kittel, T.G.F., Nemani, R.R., Running, S.W., 2000. Simulated impacts of historical land cover changes on global climate in northern winter. *Clim. Dyn.* 16, 93–105.
- Claussen, M., Brovkin, V., Ganopolski, A., 2001. Biogeophysical versus biogeochemical feedbacks on large-scale land cover change. *Geophys. Res. Lett.* 28, 1011–1014.
- Defries, R.S., Bounoua, L., Collatz, G.J., 2002. Human modification of the landscape and surface climate in the next fifty years. *Glob. Chang. Biol.* 8, 438–438.
- Dewar, R.C., 1996. The correlation between plant growth and intercepted radiation: an interpretation in terms of optimal plant nitrogen content. *Ann. Bot.* 78, 125–136.
- Dewar, R.C., 1997. A simple model of light and water use efficiency for *Pinus radiata*. *Tree Physiol.* 17, 259–265.
- Dimmeyer, P.A., Shukla, J., 1994. Albedo as a modulator of climate response to tropical deforestation. *J. Geophys. Res.* 99, 20863–20877.
- Fraedrich, K., Kleidon, A., Lunkeit, F., 1999. A green planet versus a desert world: estimating the effect of vegetation extremes on the atmosphere. *J. Clim.* 12, 3156–3163.
- Fraedrich, K., Jansen, H., Kirk, E., Luksch, U., Lunkeit, F., 2005a. The Planet Simulator: towards a user friendly model. *Z. Meteorol.* 14, 299–304.
- Fraedrich, K., Jansen, H., Kirk, E., Lunkeit, F., 2005b. The Planet Simulator: green planet and desert world. *Z. Meteorol.* 14, 305–314.
- Govindasamy, B., Duffy, P.B., Caldeira, K., 2001. Land use changes and northern hemisphere cooling. *Geophys. Res. Lett.* 28, 291–294.
- Grassl, H., 1981. The climate at maximum entropy production by meridional atmospheric and oceanic heat fluxes. *Q. J. R. Meteorol. Soc.* 107, 153–166.
- Hansen, J.E., Sato, M., Lacis, A., Ruedy, R., Tegen, I., Matthews, E., 1998. Climate forcings in the industrial era. *Proc. Natl. Acad. Sci. U. S. A.* 95, 12753–12758.
- Henderson-Sellers, A., Dickinson, R.E., Durbridge, T.B., Kennedy, P.J., McGuffie, K., Pitman, A.J., 1993. Tropical deforestation: modeling local- to regional-scale climate change. *J. Geophys. Res.* 98, 7289–7315.
- Imhoff, M.L., Bounoua, L., Ricketts, T., Loucks, C., Harriss, R., Lawrence, W.T., 2004. Global patterns in human consumption of net primary production. *Nature* 429, 870–873.
- IPCC, 2001. *Climate Change 2001: The Scientific Basis. Contribution of Working Group I to the Third Assessment Report of the Intergovernmental Panel on Climate Change.* Cambridge University Press, Cambridge, United Kingdom.
- Kleidon, A., 2002. Testing the effect of life on Earth's functioning: how Gaian is the Earth system? *Clim. Ch.* 66, 271–319.
- Kleidon, A., 2004a. Beyond Gaia: thermodynamics of life and Earth system functioning. *Clim. Ch.* 66, 271–319.
- Kleidon, A., 2004b. Global datasets of rooting zone depth inferred from inverse methods. *J. Clim.* 17, 2714–2722.
- Kleidon, A., 2004c. Optimized stomatal conductance of vegetated land surfaces and its effects on simulated productivity and climate. *Geophys. Res. Lett.* 31, L21203.
- Kleidon, A., submitted for publication. Climatic constraints on human activity and global change. *Clim. Ch.*
- Kleidon, A., Fraedrich, K., 2005. Biotic entropy production and global atmosphere–biosphere interactions. In: Kleidon, A., Lorenz, R.D. (Eds.), *Non-Equilibrium Thermodynamics and the Production of Entropy: Life, Earth, and Beyond.* Springer Verlag, Heidelberg, Germany, pp. 173–190.
- Kleidon, A., Heimann, M., 1998. A method of determining rooting depth from a terrestrial biosphere model and its impacts on the global water- and carbon cycle. *Glob. Chang. Biol.* 4, 275–286.
- Kleidon, A., Heimann, M., 1999. Deep rooted vegetation, Amazonian deforestation, and climate: results from a modelling study. *Glob. Ecol. Biogeogr.* 8, 397–405.
- Kleidon, A., Heimann, M., 2000. Assessing the role of deep rooted vegetation in the climate system with model simulations: mechanism, comparison to observations and implications for Amazonian deforestation. *Clim. Dyn.* 16, 183–199.
- Kleidon, A., Lorenz, R.D., 2005a. Entropy production by Earth system processes. In: Kleidon, A., Lorenz, R.D. (Eds.), *Non-Equilibrium Thermodynamics and the Production of Entropy: Life, Earth, and Beyond.* Springer Verlag, Heidelberg, Germany, pp. 1–20.
- Kleidon, A., Lorenz, R.D. (Eds.), 2005b. *Non-Equilibrium Thermodynamics and the Production of Entropy: Life, Earth, and Beyond.* Springer Verlag, Heidelberg, Germany.
- Kleidon, A., Fraedrich, K., Heimann, M., 2000. A green planet versus a desert world: estimating the maximum effect of vegetation on land surface climate. *Clim. Ch.* 44, 471–493.
- Kleidon, A., Fraedrich, K., Kunz, T., Lunkeit, F., 2003. The atmospheric circulation and states of maximum entropy production. *Geophys. Res. Lett.* 30, 2223.
- Kleidon, A., Fraedrich, K., Kirk, E., Lunkeit, F., 2006. Maximum entropy production and the strength of boundary layer exchange in an atmospheric general circulation model. *Geophys. Res. Lett.* 33, L06706.
- Larcher, W., 1995. *Plant Physiological Ecology*, 3rd edition. Springer Publishers, New York, NY.
- Lean, J., Rowntree, P.R., 1997. Understanding the sensitivity of a GCM simulation of Amazonian deforestation to the specification of vegetation and soil characteristics. *J. Clim.* 10, 1216–1235.
- Lorenz, R.D., Lunine, J.I., Withers, P.G., McKay, C.P., 2001. Titan, Mars and Earth: entropy production by latitudinal heat transport. *Geophys. Res. Lett.* 28, 415–418.

- Lunkeit, F., Fraedrich, K., Jansen, H., Kirk, E., Kleidon, A., Luksch, U., 2004. Planet Simulator Reference Manual. . available at <http://puma.dkrz.de/plasim>.
- Marland, G., Pielke, R.A., Apps, M., Avissar, R., Betts, R.A., Davis, K.J., Frumhoff, P.C., Jackson, S.T., Joyce, L.A., Kauppi, P., Katzenberger, J., MacDicken, K.G., Neilson, R.P., Niles, J.O., d.S. Niyogi, D., Norby, R.J., Pena, N., Sampson, N., Xue, Y., 2003. The climatic impacts of land surface change and carbon management, and the implications for climate-change mitigation policy. *Clim. Policy* 3, 149–157.
- McGuffie, K., Henderson-Sellers, A., Zhang, H., Durbridge, T.B., Pitman, A.J., 1995. Global climate sensitivity to tropical deforestation. *Glob. Planet. Change* 10, 97–128.
- Monteith, J.L., Huda, A.K.S., Midya, D., 1989. RESCAP: a resource capture model for sorghum and pearl millet. In: Virmani, S.M., Tandon, H.L.S., Alagarswamy, G. (Eds.), *Modelling the Growth and Development of Sorghum and Pearl Millet*. ICRISAT Research Bulletin, vol. 12, pp. 30–34. Patancheru, India.
- Oleson, K.W., Bonan, G.B., Levis, S., Vertenstein, M., 2004. Effects of land use change on North American climate: impact of surface datasets and model biogeophysics. *Clim. Dyn.* 23, 117–132.
- Ozawa, H., Ohmura, A., 1997. Thermodynamics of a global-mean state of the atmosphere — a state of maximum entropy increase. *J. Clim.* 10, 441–445.
- Ozawa, H., Ohmura, A., Lorenz, R.D., Pujol, T., 2003. The second law of thermodynamics and the global climate system — a review of the Maximum Entropy Production principle. *Rev. Geophys.* 41, 1018.
- Paltridge, G.W., 1978. The steady-state format of global climate. *Q. J. R. Meteorol. Soc.* 104, 927–945.
- Pavlick, R., Kleidon, A., submitted for publication. Is terrestrial productivity at its maximum for present-day conditions? *Tellus B*.
- Peixoto, J.P., Oort, A.H., de Almeida, M., Tome, A., 1991. Entropy budget of the atmosphere. *J. Geophys. Res.* 96, 10,981–10,988.
- Pielke, R.A., Marland, G., Betts, R.A., Chase, T.N., Eastman, J.L., Niles, J.O., d.S. Niyogi, D., Running, S.W., 2002. The influence of land-use change and landscape dynamics on the climate system: relevance to climate change policy beyond the radiative effect of greenhouse gases. *Philos. Trans. R. Soc. Lond., A* 360, 1705–1719.
- Polcher, J., Laval, K., 1994. A statistical study of the regional impacts of deforestation on climate in the LMD GCM. *Clim. Dyn.* 10, 205–219.
- Rojstaczer, S., Sterling, S.M., Moore, N.J., 2001. Human appropriation of photosynthesis products. *Science* 294, 2549–2552.
- Shimokawa, S., Ozawa, H., 2002. On the thermodynamics of the oceanic general circulation: irreversible transition to a state with higher rate of entropy production. *Q. J. R. Meteorol. Soc.* 107, 503–520.
- Shukla, J., Nobre, C.A., Sellers, P.J., 1990. Amazon deforestation and climate change. *Science* 247, 1322–1325.
- Sud, Y.C., Walker, G.K., Kin, J.-H., Liston, G.E., Sellers, P.J., Lau, W.K.-M., 1996. Biogeophysical consequences of a tropical deforestation scenario: a GCM simulation study. *J. Clim.* 9, 3225–3247.
- Ulanowicz, R.E., Hannon, B.M., 1987. Life and the production of entropy. *Proc. R. Soc. Lond., B* 232, 181–192.
- Vitousek, P.M., Ehrlich, P.R., Ehrlich, A.H., Matson, P.A., 1986. Human appropriation of the products of photosynthesis. *Bioscience* 36, 368–373.
- Vitousek, P.M., Mooney, H.A., Lubchenco, J., Melillo, J.M., 1997. Human domination of Earth's ecosystems. *Science* 277, 494–499.